Photosynth Res
DOI 10.1007/s11120-010-9569-1

REGULAR PAPER

Absorbance changes accompanying the fast fluorescence induction in the purple bacterium *Rhodobacter sphaeroides*

David Bína · Radek Litvín · František Vácha

Received: 28 January 2010 / Accepted: 30 May 2010

Abstract The authors present a study of the fluorescence and absorbance transients occurring in whole cells of purple nonsulfur bacterium *Rhodobacter sphaeroides* on the millisecond timescale under pulsed actinic illumination. The fluorescence induction curve is interpreted in terms of combination of effects of redox changes in the reaction center and the membrane potential. The results of this study support the view that the membrane potential act predominantly to increase the fluorescence yield. Advantages of the pulsed actinic illumination for study of the operation of the electron transport chain in vivo are discussed.

Keywords Photosynthesis · Charge separation · Membrane potential · Reaction center

D. Bína · R. Litvín · F. Vácha (✉)
Biology Centre ASCR, v.v.i, Institute of Plant Molecular Biology and Faculty of Science, University of South Bohemia, Branisovska 31, 370 05 Ceske Budejovice, Czech Republic
e-mail: vacha@jcu.cz

D. Bína
Institute of Physiology ASCR, v.v.i, Videnska 1083, 142 20 Prague, Czech Republic

Present Address:
R. Litvín
Institute of Physics, Nicolaus Copernicus University, Grudziadzka 5/7, 87-100 Torun, Poland

F. Vácha
Institute of Physical Biology, University of South Bohemia, Zamek 136, 373 33 Nove Hrady, Czech Republic

Introduction

In most photosynthetic organisms, the transition from dark to light is known to be accompanied with changes in (bacterio) chlorophyll ((B)Chl) fluorescence yield. These arise primarily due to the changes in concentrations of various redox states of components of electron transport chain, mainly reaction centers. Reaction centers (RCs) in the so-called closed state, i.e., either with the primary donor (P_{870} in purple bacteria) oxidized or the quinone acceptor (Q_A) reduced, are inefficient traps for the excitation, consequently the amount of energy lost as fluorescence (and also heat) is higher compared to the open centers (van Grondelle 1985).

Recording of the time-dependent changes of the fluorescence yield are called fluorescence induction curves. Changes that occur during the early (up to seconds) part of the induction curve reflect mostly the electron transport events within the RC, while in the later parts, the nonphotochemical processes manifest more significantly. In oxygenic photosynthesis, the stages of the fast fluorescence induction curves are nowadays usually denoted using letters OJIP (Strasser et al. 1995). These steps reflect the electron transfer from the primary donor to Q_A, from Q_A to Q_B, and reduction of the plastoquinone pool (step P). Moreover, it was shown that electric fields contribute to changes of fluorescence during the OJIP phase of the induction curve in plant chloroplasts (Bulychev et al. 1986; Dau and Bauer 1991; Dau et al. 1991; Pospíšil and Dau 2002; Vredenberg 2000; Vredenberg and Bulychev 2002, 2003).

In purple bacteria, information concerning the early steps of the fluorescence induction is scarce. It is known that on sub-second timescale, fluorescence yield increases in several steps. The phenomenological OJIP notation was applied to these steps by Strasser and Ghosh (1995), albeit

Journal : Large 11120 | Dispatch : 21-6-2010 | Pages : 7
Article No. : 9569 | ☐ LE | ☐ TYPESET
MS Code : | ☑ CP | ☑ DISK

without further analysis of the relation of the respective phases between oxygenic and anoxygenic photosynthesis.

Despite the fact that bacterial and oxygenic RC's share the basic organization of the electron transfer chain, there are fundamental differences in the electron transfer chain outside the RC. In the reaction center of photosystem 2, the oxygen-evolving complex extracts electrons from water and supplies them to the primary donor, while in the purple bacteria the reduction of the P_{870}^{+} is ultimately carried out by the mobile *c*-type cytochromes which in turn acquire the electrons via the cytochrome bc-complex from the ubiquinone pool in the membrane. Thus, the system operates in a loop in which changes of concentrations of various components of the electron transfer chain are mutually dependent. The primary consequence of such type of electron transfer is that under illumination, a bacterial sample contains a mix of two different high-fluorescence states [$P_{870}^{+}Q_A$ and $P_{870}^{-}Q_A$, e.g., (van Grondelle 1985)]. This is further complicated by the fact that fluorescence of different states of RC is modulated by the membrane potential, as was shown earlier (Steiger and Sauer 1995; Bína et al. 2009); also, effects of electric and magnetic field on charge recombination were specifically demonstrated (van der Wal et al. 1982; Kingma et al. 1983). It thus seems necessary that measurement of fluorescence is accompanied with spectroscopic measurement of the state of the electron transport chain to analyze the processes underlying the fluorescence induction curve.

We present description of the early steps of the kinetics of absorbance changes and fluorescence in whole cells of purple bacterium *Rhodobacter (Rb.) sphaeroides* on the millisecond to second timescale under pulsed actinic illumination. This study complements the earlier study concerning the spectroscopic signatures of the in vivo operation of the bacterial electron transport chain (Bína et al. 2009).

Materials and methods

Purple nonsulfur bacterium *Rb. sphaeroides*, strain Y, was grown anaerobically in Sistrom medium (Sistrom 1962) in 25-ml screw top flasks under incandescent lamp providing irradiance of about 150 μmol m^{-2} s^{-1} at the surface of the cultivation vessel. Cells were harvested after reaching optical density (OD) of 1 at 700 nm, washed with 20 mM K-phosphate buffer of pH 6.8, and resuspended in fresh Sistrom medium to the OD_{700} of 0.2 (6 μmol(BChl) l^{-1}) estimated after (Siefert et al. 1978). Prior to the measurement, the cells were bubbled by nitrogen and placed in a plastic cuvette and then sealed to keep anaerobic conditions during measurement. Measurements were conducted using the laboratory-built multichannel kinetic absorption spectrometer, which is described in detail elsewhere Bína et al. (2006). While our instrument is well suited for parallel measurements of fluorescence and absorbance on the timescale above hundreds of millisecond under continuous actinic illumination, its application for the measurement of fast induction curves required a modification of the experimental approach.

Here, we used a light-emitting diode unit which is a component of the fluorimeter FL100 (PSI, Czechia) as the source of actinic flashes. The unit was fitted with infrared diodes with emission maxima at 890 and 850 nm. The duration of actinic flashes was 10 μs in most experiments. Since the instrument utilizes a high-pressure Xenon flash lamp with the repetition time of 30 ms, for the measurement of induction on millisecond time scales, the pump–probe approach had to be employed. The sample was submitted to a series of actinic flashes after which a measuring flash was applied to detect spectral changes. The number of actinic pulses was increased in each run, and the induction curves were constructed from these subsequent runs.

Fluorescence induction curves were recorded in separate runs, using the same pulse setting as the absorbance kinetics, but in single measurement instead of the pump–probe point by point mode. Fluorescence was detected using a PIN diode (PSI, Czechia), and a set of blue (460 nm) light-emitting diodes served as a source of measuring flashes. The background signal that arose from the actinic IR pulses hitting the detector was recorded in a separate experiment without measuring flashes and later subtracted from the fluorescence measured with the measuring flashes.

All the measurements were separated by a dark interval of duration such that both fluorescence and absorbance changes decayed, and thus, each consequent run was performed on a dark-adapted sample.

The slow induction curves presented for comparison in the following section were measured in separate experiments using the setup exactly as described in (Bína et al. 2009), with a halogen lamp (Fiber-Lite A3200, Dolan-Jenner, USA), switched using a shutter with the opening halftime of 0.5 ms (Uniblitz VMD-D1, Vincent Associates, USA). Parallel detection of absorbance and fluorescence was used in these measurements. Since the measurement of the fast transients required a considerable change of the experimental setup, switching between the pulsed and continuous mode was not possible. Where provided, continuous traces come from different samples than the pulse-induced transients.

Results and discussion

The fluorescence induction curve

In Fig. 1, a fast fluorescence induction curve as measured on the whole cells of *Rb. sphaeroides* under a series of

Journal : Large 11120 | Dispatch : 21-6-2010 | Pages : 7
Article No. : 9569 | LE | TYPESET
MS Code : | CP | DISK

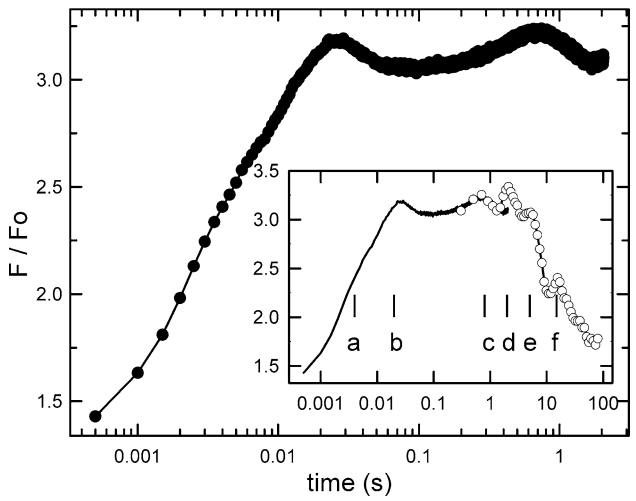

Fig. 1 Fast fluorescence induction curve in *Rb. sphaeroides* measured with pulsed actinic illumination. *Inset*: the whole fluorescence transient. The trace labeled with *empty circles* was measured using the continuous illumination of 2000 μmol m^{-2} s^{-1}

10 μs actinic flashes spaced by 500 μs is shown. In the inset, the whole fluorescence transient covering the time range up to 80 s is presented. The slow part was taken from the measurement performed under continuous illumination. The correspondence of the overlapping region of the fast and slow curves is not perfect—namely, the fast induction curve suggests a slightly later appearance of the peak around the 2nd second as compared to the trace recorded with the continuous illumination, which is expectably due to the different modes of illumination and also the fact that the recordings come from different samples. By comparison of a larger number of induction curves, we concluded that the assignment of the phases in the fast and slow induction curves given below reflects the common characteristics of the whole fluorescence induction curve in *Rb. sphaeroides*, although the precise positions and the relative amplitudes of the phases differ among samples. Also, as seen in Fig. 1, the fastest component of the induction curve, around 4 ms does not appear as well-resolved peak, and its exact characterization is thus quite difficult at present.

At least seven separate steps can be discerned in the joined graph of fast and slow fluorescence induction curves; these are labeled in Fig. 1. We decided to abandon the OJIP formalism in favor of the neutral alphabetical labeling because correspondence of fluorescence transients in oxygenic and bacterial photosynthesis is not yet clear, and these labels might cause confusion. The typical times of the phases of fluorescence induction curves in *Rb. sphaeroides* are

Step	Fo	a	b	c	d	e	f
Time	Dark	4 ms	20 ms	0.8 s	1–3 s	5–7 s	10–15 s

Since the phases "d"–"f" were discussed in the earlier study (Bína et al. 2009), here we will concentrate only on the fast part of the transient. In order to obtain information about the underlying processes, the absorbance changes measurements were used.

Absorbance changes

Overview

In brief, the light minus dark difference spectrum in the range from 460 to 660 nm contains three types of features: (i) transient bleaching of the BChl Q_x absorption band around 600 nm and of *c*-type cytochrome band around 550 nm, which result from oxidation of the chromophores; (ii) changes between 460 and 520 nm predominantly due the electrochromic shift of the absorption bands of carotenoids that arise in response to external electric fields. This absorption change is indicative of the membrane potential that builds up as a consequence of not only proton translocation but also of the primary donor oxidation (presence of P_{870}^+); and (iii) the spectrum as a whole shifts upward in response to illumination. The effect is more pronounced toward the short wavelength end of the spectrum and can be ascribed to an increase of light scattering. As noted before (Bína et al. 2009), it is necessary to perform a correction of the difference spectra for the effect of scattering to obtain correct values for absorbance changes. Namely, a linear function that intersected the spectra at 580 and 660 nm was subtracted from the data.

The three types of absorbance changes described above can be effectively used to describe different fast processes on bacterial photosynthetic membrane. By measuring the amplitude of the negative bands at 553 and 600 nm, amounts of oxidized *c*-type cytochromes and of P_{870}^+ can be estimated, respectively. Changes of the membrane potential can be followed using the peak–trough amplitudes of the electrochromic bandshift (e.g., $\Delta A_{490-510}$). And finally, extent of the scattering can be quantified by measuring absorbance at 660 nm, that is, outside of the region of pigment absorption.

Correction of the membrane potential

If the electrochromic shift of carotenoids is to be used as a measure of the membrane potential due to proton translocation, then it has to be corrected for the effect of a local charge of the P_{870}^+. We used the following procedure, which has been described (Bína et al. 2009). In Fig. 2, we present a plot of amplitudes of single flash-induced electrochromic bandshift versus the amount of P_{870}^+. This graph contains data from 12 samples, actinic flashes were,

Journal : Large 11120 Dispatch : 21-6-2010 Pages : 7
Article No. : 9569 LE TYPESET
MS Code : CP DISK

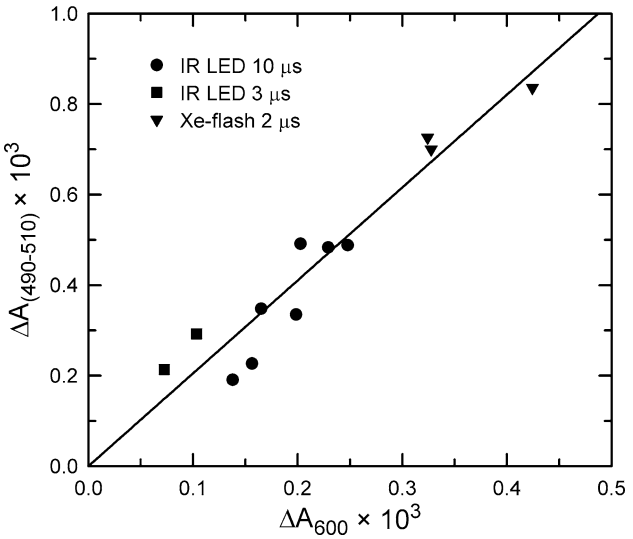

Fig. 2 Flash-induced amplitude of the carotenoid electrochromic bandshift ($\Delta A_{490–510}$) plotted against the amplitude of the bleaching of the P_{870} BChl *a* band at 600 nm ($-\Delta A_{602}$) in whole cells of *Rb. sphaeroides*. Each point corresponds to a different sample. Sources of actinic pulses are listed in the legend

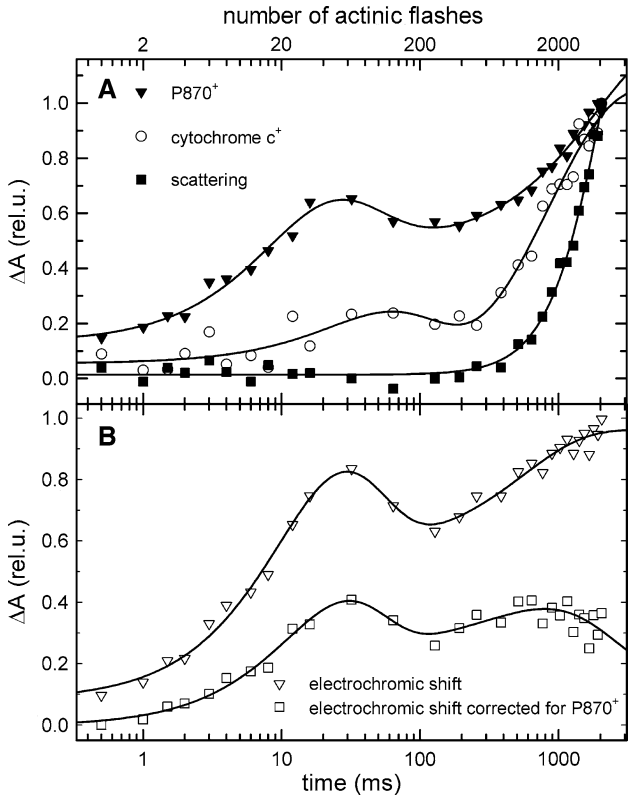

Fig. 3 Kinetics of absorbance changes in whole cells of *Rb. sphaeroides* during pulsed actinic illumination (10 μs pulses). **A** (*solid triangles*) oxidized primary donor ($-\Delta A_{602}$) (*open circles*) oxidized cytochrome *c* (*solid squares*) kinetics of increase of the light scattering, detected as amplitude of baseline shift of difference spectra at 660 nm. **B** (*open triangles*) kinetics of the membrane potential, detected by the electrochromic shift of carotenoids ($\Delta A_{490–}$ ΔA_{510}) (*open squares*) the same kinetics after correction for primary donor contribution. Smooth lines are sums of exponential functions

as indicated, provided by LEDs (10 and 3-μs duration) and Xe-flash lamps (2 μs duration). For single-turnover conditions, the electrochromic bandshift is proportional to the amount of P_{870}^+, assuming that there is no membrane potential immediately after the flash. Consequently, by dividing the absorbance amplitudes measured after the first flash, one obtains the correction factor (q) for P_{870}^+: $q = \Delta A_{490–510}/(-\Delta A_{600})$.

For the whole kinetics, it follows that the absorption change proportional to the membrane potential, cleared of the P_{870}^+ effect equals: $\Delta A_{490–510}(time) - [-\Delta A_{600}(time)] \times q$.

Kinetics

In Fig. 3, we show kinetics of the P_{870}^+, oxidized cytochrome *c* and light scattering (*A*), and kinetics of membrane potential ("raw" as well as corrected for the P_{870}^+ effect, in Fig. 3B). Note that all kinetics presented in the following section were reconstructed from a sequence of pump–probe measurements with increasing number of flashes as described in Material and methods section. Numbers of flashes are also indicated (upper axis).

Despite the fact that pictured kinetics were induced by a series of flashes, no oscillatory behavior was observed. Thus, this light regime, i.e., 10-μs flashes fired at 2 kHz frequency simulate continuous illumination. As shown, kinetics of P_{870}^+ and raw electro-chromic shift can be satisfactorily fitted with a sum of three exponentials; however, at this point we present the fit mostly as a guide to the eye, its physical interpretation being beyond the scope of this study. They start with a mono-exponential rise to a local maximum around 30 ms, followed by a small decrease, and a substantial slower, exponential rise in times from 100 ms on. As shown earlier, the transients reach maxima in times between 2 and 4 s (Bína et al. 2009). As for the cytochrome c^+, its course follows the P_{870}^+ with a slight delay. The corrected kinetics of the membrane potential shows two distinct peaks, around 30 and 1000 ms. The position of the first peak is close to the maximum of the membrane potential observed after a single-turnover flash (Bína et al. 2009), and probably reflects the first turnover of the cytochrome *bc*-complex. On the other hand, the formation of the Q_BH_2 in the RC certainly influences the kinetics of the membrane potential as well. Unfortunately, signal-to-noise ratio of the kinetics of cytochrome c^+ does not permit a more precise analysis of the cytochrome action at this point. In the kinetics of scattering, there is an apparent lag phase at the beginning. The

Journal : Large 11120 Dispatch : 21-6-2010 Pages : 7
Article No. : 9569 LE TYPESET
MS Code : CP DISK

increase of scattering starts roughly at 200 ms and parallels the increase of P_{870}^+ and oxidized cytochrome.

As we showed above, there is rather a clear continuity between the fast (pulsed) and the slow (continuous) induction curves of fluorescence. We illustrate this fact also for the absorbance changes, using the example of the kinetics corresponding to P_{870}^+;(Fig.4). As seen here, three distinct phases can de discerned in the whole kinetics of P_{870}^+, proceeding in tens of milliseconds, second, and tens of seconds scale, respectively.

Comparison of fluorescence induction curve with absorbance data The rise of fluorescence yield during the first 10 ms of the induction is not accompanied by proportional increase of P_{870}^+. This indicates that this phase is predominantly due to the accumulation of $P_{870}^-Q_A$ state, while the P_{870}^+ is still effectively removed by the action of cytochromes. This would suggest that the subset of RCs that initially contain reduced cytochromes in the vicinity is responsible for this part of the induction curve. The peak around 20 ms then apparently parallels the accumulation of P_{870}^+. Interestingly, the subsequent course of the fluorescence induction curve does not follow P_{870}^+ accumulation, but rather the corrected membrane potential (as shown in Fig. 3B). Thus the following maximum at about 800 ms is probably due this effect. The positive effect of the membrane potential is in agreement with our previous observations (Bína et al. 2009). Since the effect of the electric field on fluorescence is especially marked at the $P_{870}^-Q_A$ state (Bína et al. 2009), we suggest that within hundreds of milliseconds, most RCs already have their Q_A reduced. The positive effect of the membrane potential on fluorescence is supported by the fact that application of uncoupler gramicidin lowers the fluorescence yield by about 20% (not shown). It suggests that the shape of the fluorescence induction curve is determined by the concentrations of the various redox states of RC as well as by the effect of the membrane potential on these states. It is obvious that measurement of fluorescence induction alone is not sufficient to obtain exact information on the electron transfer around the RC.

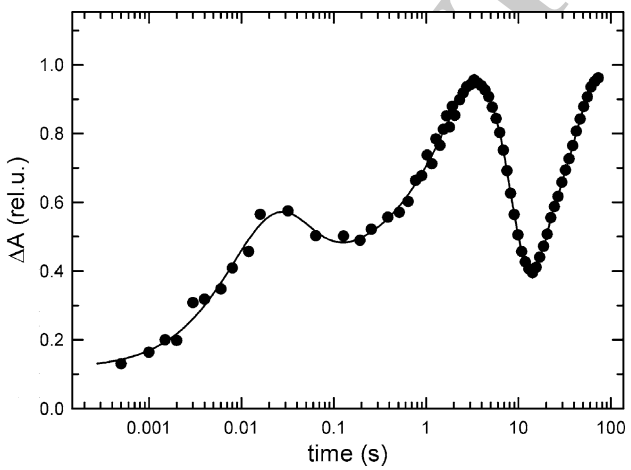

Fig. 4 The whole induction curve of oxidized primary donor in *Rb. sphaeroides*. The trace was constructed by combining the kinetics of Fig. 3 with data obtained using the continuous actinic illumination as in the Fig. 1

General considerations

Although the combination of fluorescence and absorbance provides information on redox state of most of the components of the electron transport chain, we will not at this point attempt to provide a concise model for operation of the electron transfer. There is an inherent difficulty in constructing such model for the native membrane of purple bacteria, which stems from the cyclic operation of the electron transfer. That is, a connection between the electron transfer from the RC toward the cytochrome bc_1 complex via the ubiquinone pool and reduction of the P_{870}^+ by the mobile cytochrome c_2. Thus, increased rate of the electron flow to the ubiquinones will later be reflected in the increased availability of the reduced cytochrome c_2. Kinetic properties of this feedback will depend not only on the inherent thermodynamical properties of the electron transfer reaction, but also on the local spatial organization of the protein complexes.

The presence of changes of the light-scattering points to the possibility that structural changes of the membrane take place under illumination. These may bring about changes in the relative position of components of the electron transfer chain or mechanical properties of the membrane. In such case, changes of the rate constants of the particular reactions will follow, adding another level of complexity to the problem. On the other hand, as pointed out recently, the diffusion rates might not be the crucial factor determining the rates of the electron transfer reactions (Geyer and Helms 2006).

Another important question is the effect of the reverse electron flow on the state of the ubiquinone pool. This process reduces NAD^+ by ubiquinol at the expense of membrane potential (Imhoff 1995). The ubiquinones are reduced by the succinate dehydrogenase. While theoretical study of the overall operation of the electron transport chain was recently provided (Klamt et al. 2008), real-time kinetic data on relation of the reverse electron flow to the photosynthetic electron transfer are not available.

The application of the pulsed actinic illumination offers one interesting possibility for study of these complex problems outlined above. While the actinic effect can be compared to that of the continuous illumination, as shown above, there is also possibility to measure the decays of the absorbance changes between actinic pulses to extract more information concerning the rates of the electron transport

Journal : Large 11120 Dispatch : 21-6-2010 Pages : 7
Article No. : 9569 LE TYPESET
MS Code : CP DISK

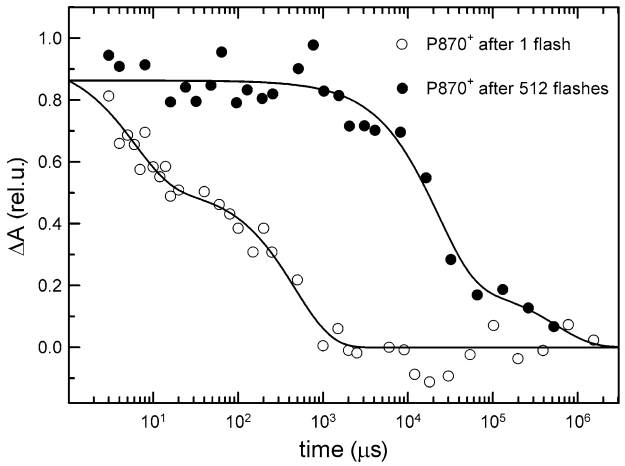

Fig. 5 Decay of the oxidized primary donor: (*open circles*) after single actinic flash; (*solid circles*) after 512 actinic flashes (256 ms). Each decay was fitted with a sum of two exponentials; for details see text

reactions. In order to illustrate this, we present kinetics of the decay of light-induced P_{870}^{+}, Fig. 5. It shows the decay after a single actinic flash (open circles) and after 512 actinic flashes (solid circles) that is, about 250 ms after the start of the induction. Both decays can be fitted by a sum of two exponentials, which we present to facilitate orientation in the figure. In the single-turnover case, the oxidized P_{870}^{+}'s are fully reduced within a millisecond, which indicates a readily available pool of reduced cytochromes in the vicinity of the RCs. For the multiple-turnover case, the majority of the P_{870}^{+} is reduced with the rate constant of about 1/(22 ms). This is not very far from the value of 13 ms estimated for a round trip of the cytochrome c_2 by Geyer and Helms (2006) for chromatophores. On the other hand, the kinetic data show that it takes atleast 1 min (see e.g., Fig. 4 and Bína et al. 2009) before the electron flows within the electron transfer chain reach equilibrium, thus the steady state-derived assumptions have to be taken with caution.

In this study, we utilized the present experimental setup of the pump–probe measurement to construct the kinetics of absorbance changes point by point. This is tedious and time consuming as well as prone to artifacts due to repeated exposure of the sample. As we attempted to ensure that the dark periods between repeated series of actinic flashes were long enough for any accumulation of absorbance changes to disappear, obtaining a complete transient was a matter of hours, which is clearly not very useful. Hence, for further studies concerning these processes, it would be beneficial to apply measurements only at selected wavelengths, provided, for example, by LEDs. Application of limited range of wavelengths for detection would lower the overall actinic effect of the measuring light. Also, with proper filtering, there would be no need for wavelength-resolved detection which will allow a higher sampling frequency for fast transients.

Conclusion

The sub-second section of the fluorescence induction curve in purple bacterium *Rb. sphaeroides* consists of three discernible phases, occurring at about 4, 20, and 800 ms, respectively. By comparison with the kinetics of absorbance changes due to primary donor oxidation and membrane potential build-up, we deduced the possible major factors behind these phases: the earliest phase is mainly due to Q_A reduction, while both the amounts of P_{870}^{+} and the membrane potential are low; however, the present data do not allow very precise resolution of the fastest parts of the induction curve. The following phase, around 20 ms, coincides with the local maximum of P_{870}^{+} accumulation. Thereafter, the fluorescence yield parallels mainly the time course of the membrane potential.

This study, to our knowledge is the first to offer characterization of the processes underlying the fast changes of the fluorescence yield in purple bacteria. We were able to obtain data concerning both the electron transfer around RC and the build-up of the membrane potential on the sub-second time scales in whole cells. Such study represents a necessary step in the way toward understanding of the operation of the photosynthetic machinery under natural physiological conditions.

Acknowledgments The authors would like to acknowledge the financial support of the Ministry of Education, Youth and Sports of the Czech Republic under grant Nos. MSM6007665808, MSM6007665801, AV0Z50510513, and GAAV A608170603.

References

Bína D, Litvín R, Vácha F, Šiffel P (2006) New multichannel kinetic spectrophotometer-fluorimeter with pulsed measuring beam for photosynthesis research. Photosynth Res 88:351–356

Bína D, Litvín R, Vácha F (2009) Kinetics of in vivo bacteriochlorophyll fluorescence yield and the state of photosynthetic apparatus of purple bacteria. Photosynth Res 99:115–125

Bulychev AA, Niyazova MM, Turovetsky VB (1986) Electro-induced changes of chlorophyll fluorescence in individual intact chloroplasts. Biochim Biophys Acta 810:218–225

Dau H, Bauer K (1991) Electric-field effect on chlorophyll fluorescence and its relation to photosystem-ii charge separation reactions studied by a salt-jump technique. Biochim Biophys Acta 1098:49–60

Dau H, Windecker R, Hansen U-P (1991) Effect of light-induced-changes in thylakoid voltage on chlorophyll fluorescence of aegopodium-podagraria leaves. Biochim Biophys Acta 1057: 337–345

Geyer T, Helms V (2006) A spatial model of the chromatophore vesicles of *Rhodobacter sphaeroides* and the position of the cytochrome bc(1) complex. Biophys J 913:921–926

Journal : Large 11120 | Dispatch : 21-6-2010 | Pages : 7
Article No. : 9569 | LE | TYPESET
MS Code : | CP | DISK

Imhoff JF (1995) Taxonomy and physiology of phototrophic purple and green sulphur bacteria. In: Blankeship RE, Madigan MT, Bauer CE (eds) Anoxygenic photosynthetic bacteria. Kluwer, Dordrecht, pp 1–15

Kingma H, Duysens LNM, Van Grondelle R (1983) Magnetic fieldstimulated luminiscence and a matrix model for energy transfer. A new method for determining the redox state of the first quinone acceptor in the reaction center of whole cells of Rhodospirillum rubrum. Biochim Biophys Acta 725:434–443

Klamt S, Grammel H, Straube R, Ghosh R, Gilles ED (2008) Modelling the electron transport chain of purple non-sulfur bacteria. Mol Syst Biol 4:156

Pospíšil P, Dau H (2002) Valinomycin sensitivity proves that light-induced thylakoid voltages result in millisecond phase of chlorophyll fluorescence transients. Biochim Biophys Acta 1554:94–100

Siefert E, Irgens RL, Pfennig N (1978) Phototrophic purple and green bacteria in a sewage treatment plant. Appl Environ Microbiol 35:38–44

Sistrom WR (1962) The kinetics of the synthesis of photopigments in *Rhodopseudomonas sphaeroides*. J Gen Microbiol 28:607–616

Steiger J, Sauer K (1995) Electric field effects on the steady-state fluorescence emission of *Rb. sphaeroides* chromatophores. In: Mathis M (ed) Photosynthesis: from light to biosphere. Kluwer, Dordrecht, pp 735–738

Strasser RJ, Ghosh R (1995) The fast fluorescence transient of *Rhodospirillum rubrum* is polyphasic of the type O-K-J-I-P. In: Mathis M (ed) Photosynthesis: from light to biosphere. Kluwer, Dordrecht, pp 915–918

Strasser RJ, Srivastava A, Govindjee (1995) Polyphasic chlorophyll *a* fluorescence transient in plants and Cyanobacteria. Photochem Photobiol 61:32–42

van der Wal HN, van Grondelle R, Kingma H, van Bochove AC (1982) The effect of a membrane potential on the kinetics of the nanosecond recombination luminiscence and the reaction center triplet yield in *Rhodospirillum rubrum* chromatophores. FEBS Lett 145:155–159

van Grondelle R (1985) Excitation energy transfer, trapping and annihilation in photosynthetic systems. Biochim Biophys Acta 811:147–195

Vredenberg WJ (2000) A three-state model for energy trapping and chlorophyll fluorescence in photosystem II incorporating radical pair recombination. Biophys J 79:26–38

Vredenberg WJ, Bulychev AA (2002) Photo-electrochemical control of photosystem II chlorophyll fluorescence in vivo. Bioelectrochemistry 57:123–128

Vredenberg WJ, Bulychev AA (2003) Photoelectric effects on chlorophyll fluorescence of photosystem II in vivo. Kinetics in the absence and presence of valinomycin. Bioelectrochemistry 60:87–95

Journal : Large 11120 | Dispatch : 21-6-2010 | Pages : 7
Article No. : 9569 | ☐ LE | ☐ TYPESET
MS Code : | ☑ CP | ☑ DISK